



Modification of a first-generation solid oxide fuel cell cathode with Co_3O_4 nanocubes having selectively exposed crystal planes

Xi Xu¹ · Chao Wang¹ · Marco Fronzi² · Xuehua Liu¹ · Lei Bi¹ · X. S. Zhao^{1,3}

Received: 31 July 2019 / Accepted: 13 August 2019 / Published online: 22 August 2019
© The Author(s) 2019

Abstract

Co_3O_4 nanocubes with exposed (001) planes were prepared and employed for use as first-generation Sr-doped LaMnO_3 (LSM) cathodes in solid oxide fuel cells to improve the cell performance. Theoretical simulations suggest that the Co_3O_4 (001) plane has the smallest oxygen adsorption and oxygen dissociation energies compared with other planes, thus favouring cathode reactions in solid oxide fuel cells (SOFCs). Experimental studies consistently demonstrate that a cell using an LSM cathode made with Co_3O_4 nanocubes with selective (001) surfaces exhibits a peak power density of 500 mW cm^{-2} at $600 \text{ }^\circ\text{C}$, while the power output for a cell using unselective (commercial) Co_3O_4 nanoparticles is only 179 mW cm^{-2} at the same temperature. The electrochemical study indicates that the use of Co_3O_4 nanoparticles with exposed (001) surfaces obviously accelerates the cathode reactions and thus decreases the polarisation resistance, which is the key to improving fuel cell performance. This study demonstrates the feasibility of using the crystal planes of metal oxides to improve the fuel cell performance and provides a new way to design SOFC cathodes.

Keywords Co_3O_4 · Cathode · Density functional theory · Nanocubes · Solid oxide fuel cells

Introduction

Solid oxide fuel cells (SOFCs), which can directly convert chemicals into electricity, are regarded as low-pollution devices that can be used to generate electricity [1]. Cathodes are a key component of SOFCs and have received considerable attention, as they significantly govern SOFC performance [2–4]. Sr-doped LaMnO_3 (LSM) is a first-generation cathode material used in SOFCs, and it is also one of the

most traditional SOFC cathode materials that has been successfully employed in commercial SOFC systems [5]. However, LSM is regarded as a good cathode material for applications in SOFCs at high temperatures (above $800 \text{ }^\circ\text{C}$), but it is not an appropriate cathode material for use in SOFCs at intermediate temperatures (approximately, $600 \text{ }^\circ\text{C}$) due to its pure electronic conductivity without any apparent ionic conductivity [6]. Therefore, the design of nanostructured LSM cathodes [7] and the use of new materials with electron and oxygen ion mixed conductivity [8, 9] as cathodes in SOFCs at intermediate temperatures have been proposed.

Alternatively, the addition of traditional metal oxides to cathodes has been demonstrated to be beneficial for improving the cathode performance. Zhang et al. [10] have added a Co_3O_4 layer to the $\text{Sm}_{0.5}\text{Sr}_{0.5}\text{CoO}_{3-\delta}$ cathode and found that the fuel cell performance could be doubled compared with the pure SSC cathode. Zhang et al. [11] coated a $\text{BaCe}_{0.4}\text{Sm}_{0.2}\text{Fe}_{0.4}\text{O}_3$ cathode with cobalt oxide, improving the fuel cell performance at intermediate temperatures. Li et al. [12] also found that the addition of Co_3O_4 to an LSM cathode can improve the cathode performance, although the performance is still mediocre at intermediate temperatures. It is generally accepted that Co_3O_4 is a good oxygen reduction catalyst for use in SOFCs operated at intermediate

Xi Xu and Chao Wang have contributed equally to this paper.

✉ Marco Fronzi
marco.fronzi@mail.xjtu.edu.cn

✉ Lei Bi
bilei@qdu.edu.cn; bilei81@gmail.com

¹ Institute of Materials for Energy and Environment, College of Materials Science and Engineering, Qingdao University, Ningxia Road No. 308, Qingdao 266071, China

² State Key Laboratory of Multiphase Flow in Power Engineering, International Research Centre for Renewable Energy, Xi'an Jiaotong University, Xi'an, China

³ School of Chemical Engineering, The University of Queensland, St Lucia, QLD 4072, Australia

temperatures. However, note that these studies used ordinary Co_3O_4 particles and did not investigate the effect of selectively exposing different Co_3O_4 planes on the cathode reactions. Research in the catalysis field has demonstrated that the different Co_3O_4 planes have a significant impact on their activity for catalytic reactions, such as CO oxidation and CH_4 combustion [13–15]. Therefore, it is reasonable to assume that the electrochemical performance of the cell could be improved by exposing a specific plane of Co_3O_4 instead of using ordinary Co_3O_4 particles, although such an attempt has not been performed in the SOFC community.

In this paper, a theoretical simulation was performed to investigate the adsorption and dissociation of oxygen on different Co_3O_4 planes, aiming to find a suitable plane for SOFC cathode reactions. Subsequently, Co_3O_4 nanoparticles with selectively exposed planes were synthesized and employed in the LSM cathode of an SOFC. The electrochemical performance of a cell made with an LSM cathode composed of Co_3O_4 nanocubes with specific exposed planes was studied and compared with that of a cell made with an LSM cathode composed of regular Co_3O_4 nanoparticles.

Experimental

All calculations were performed using density functional theory (DFT) [16] and were implemented using VASP (Vienna ab initio simulation package) [17, 18]; the generalized gradient approximation (GGA) was performed using the Perdew–Burke–Ernzerhof approach to approximate the exchange–correlation term. Here, the core–valence interaction is described by the projector-augmented wave method [19]. To correctly represent the electronic structure, the Hubbard correction was included [20, 21], using a U_{eff} (Co-3d) value of 3.32 eV [22]. The plane wave cutoff energy was set to 520 eV, whereas the Brillouin zone was described by a $1 \times 1 \times 1$ K-point gamma-centred mesh. To study the surface properties, a periodic slab consisting of a 2×2 repetition of the unit cell was built and had eight atomic layers and a 15 Å vacuum gap. The convergence criteria for the energy and force were set to 10^{-5} eV and 0.02 eV \AA^{-1} , respectively, during geometry optimization. The dissociation barriers on the (001), (110) and (111) facets were calculated by using climbing image nudged elastic band (CI-NEB) method [23], where the convergence criteria for energy and force were 10^{-5} eV and 0.02 eV \AA^{-1} , respectively.

The Co_3O_4 nanocubes were prepared by a hydrothermal process according to the literature [13, 24] with some modifications. Briefly, an NaOH solution (0.30 g NaOH + 10 mL distilled water) was first dispensed into a $\text{Co}(\text{NO}_3)_2$ solution (8.73 g $\text{Co}(\text{NO}_3)_2 \cdot 6\text{H}_2\text{O}$ + 20 mL distilled water), and the resulting solution was placed in a Teflon liner and stirred for 30 min. Subsequently, the Teflon liner was put into a stainless

steel autoclave and then treated at $180 \text{ }^\circ\text{C}$ for 3 h. After cooling it down to room temperature, the obtained product was filtered, washed several times with ethanol and deionized water and further dried at $60 \text{ }^\circ\text{C}$. Finally, Co_3O_4 was obtained after firing at $500 \text{ }^\circ\text{C}$ for 3 h in air.

The cathode was used in an $\text{Sm}_{0.2}\text{Ce}_{0.8}\text{O}_2$ (SDC)-based fuel cell system. The SDC powder was synthesized by a combustion method, and the preparation details can be found elsewhere [25]. The SDC powder was calcined at $700 \text{ }^\circ\text{C}$ for 3 h to obtain a pure phase powder. The SDC powder was mixed with NiO and starch at a weight ratio of 2:3:1 (SDC powder:NiO:starch) and the resulting mixture was used as the anode powder. For preparing the anode powder, SDC, NiO and starch powders were mixed in an ethanol solution and mixed with ball milling. After milling for 24 h, the solution was put in an oven at $70 \text{ }^\circ\text{C}$ to evaporate ethanol. The dried powder was collected as the composite anode powder. The SDC-based half cells were prepared by co-pressing and co-sintering methods and sintered at $1450 \text{ }^\circ\text{C}$ for 6 h. Then, an $\text{La}_{0.8}\text{Sr}_{0.2}\text{MnO}_{3-6}$ (LSM20)–SDC cathode slurry was deposited on the surface of the sintered SDC electrolyte and then co-fired at $1000 \text{ }^\circ\text{C}$ for 3 h to attach the cathode layer to the electrolyte, forming a complete cell with the structure of NiO–SDC(anode)/SDC(electrolyte)/LSM–SDC(cathode). The LSM20 powder was also synthesized by a combustion method, as mentioned above. To study the effect of exposing different Co_3O_4 surfaces on the fuel cell performance, the synthesized plane selective Co_3O_4 nanoparticles were dispersed in distilled water by using ultrasonic dispersion. Then, the dispersed Co_3O_4 particles were infiltrated into the porous LSM20–SDC composite cathode layer until the Co_3O_4 :LSM20–SDC weight ratio was 1:5, forming the LSM20–SDC– Co_3O_4 (plane selective) cathode layer. For comparison, a similar procedure was performed to infiltrate the same amount of commercial Co_3O_4 nanoparticles into the LSM20–SDC cathode layer. The commercial Co_3O_4 nanoparticles were purchased from Aladdin (Product no. C131625), and the particle size was approximately 100 nm. The material was directly used without further treatment. After the deposition of the Co_3O_4 particles, both cells were fired at $800 \text{ }^\circ\text{C}$. The fuel cell tests were performed using wet hydrogen as the fuel and static air as the oxidant. The electrochemical performance, including I–V and electrochemical impedance spectroscopy (EIS), was measured by using an electrochemical workstation (CHI 760E CH Instruments). The morphologies of the cells were observed using a field-emission scanning electron microscope (FESEM, JSM-7800F).

Results and discussion

Figure 1 shows a schematic illustrating the oxygen adsorption and dissociation at the Co_3O_4 (001) surface. It is known that in oxygen reduction mechanisms, the adsorption and

dissociation of molecular oxygen are crucial steps [26], and a decrease in the energies of either of these processes will be beneficial for cathode reactions. Here, we decided to perform a comparative study in which three facets, namely, the (001), (110) and (111) crystal planes, are considered. These three surfaces are selected, since they are thermodynamically stable terminations of Co_3O_4 [14, 24]. Our results for the oxygen adsorption and oxygen dissociation energies of the (001), (110) and (111) surfaces are summarized in Table 1. The calculated oxygen adsorption energy for the Co_3O_4 (001) surface is negative and has a value of -1.905 eV, indicating that oxygen adsorption is thermodynamically favourable on (001) surfaces. In contrast, the calculated oxygen adsorption energy is positive for the (110) and (111) surfaces, suggesting that this process

Table 1 Oxygen adsorption and dissociation energies for Co_3O_4 with (001), (110) and (111) surfaces

	(001)	(110)	(111)
Adsorption (eV)	-1.905	1.389	1.268
Dissociation (eV)	1.69	4.02	3.58

is unfavourable. For adsorbed O_2 , a dissociation will occur with an energy barrier of 1.69, 4.02 and 3.58 eV at the (001), (110) and (111) surfaces, respectively. Our results indicate that the (001) surface clearly has the lowest energy barrier, which indicates that the barrier for oxygen dissociation from the Co_3O_4 (001) surface is the lowest among the three facets. In summary, our results suggest that the adsorption and

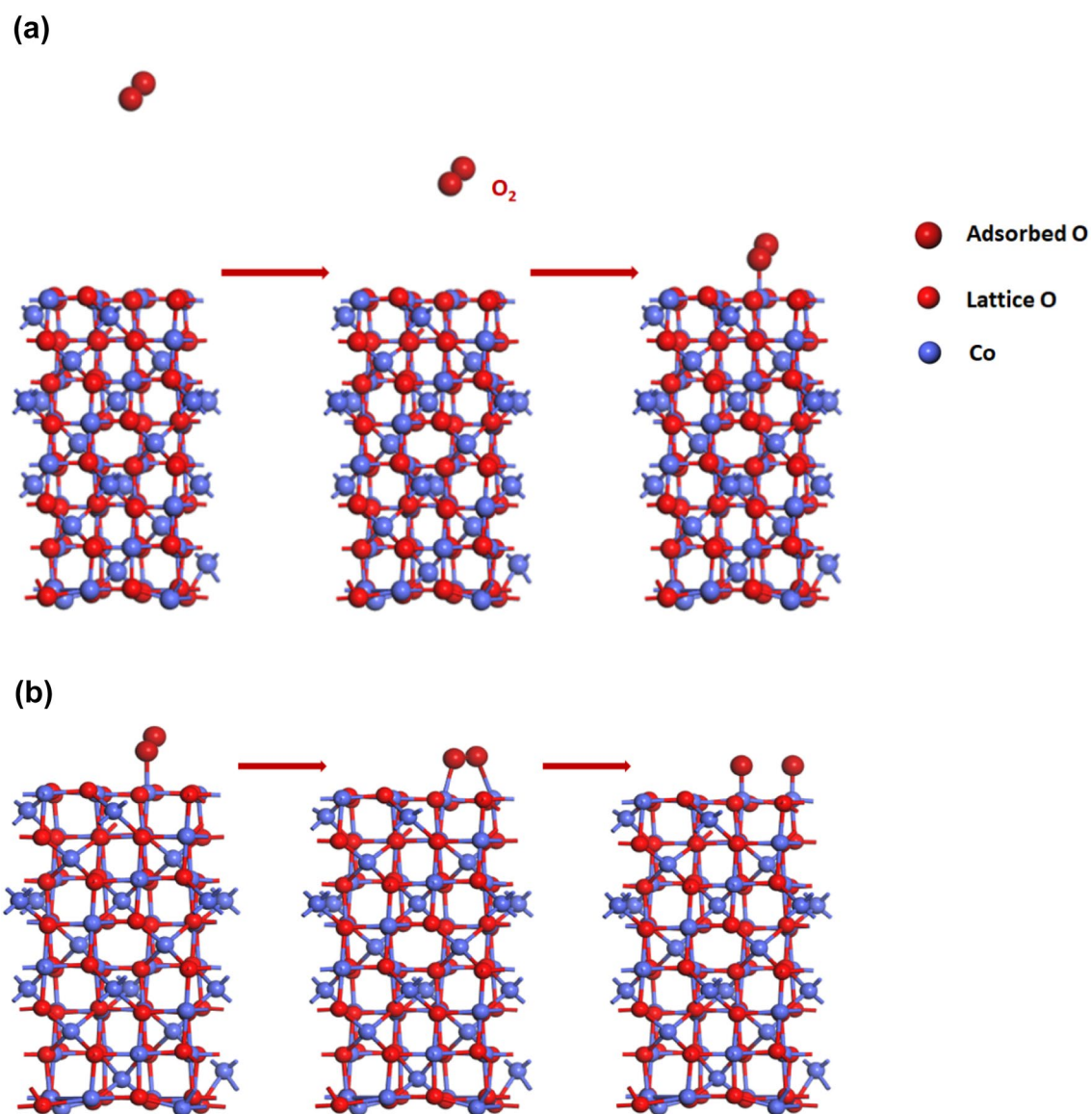


Fig. 1 Schematics for **a** oxygen adsorption and **b** oxygen dissociation on Co_3O_4 surfaces

dissociation of oxygen will be favourable only at the Co_3O_4 (001) surface, and the improved adsorption and dissociation of oxygen could facilitate the cathodic oxygen reduction reaction (ORR) [27].

Therefore, it is reasonable to expect that the Co_3O_4 (001) plane could promote fuel cell performance due to its improved catalytic activity for ORRs. To demonstrate this hypothesis, the Co_3O_4 nanocubes with exposed (001) surfaces were synthesized by a hydrothermal process, and the synthesized powder was characterized before it was used in the fuel cells. Figure 2a shows a TEM micrograph of the synthesized Co_3O_4 nanoparticles with selective (001) planes. The particles are regular cubes with particle sizes of approximately 100–150 nm. As shown in Fig. 2b, high-resolution TEM (HRTEM) was used to measure the lattice spacing,

which is approximately 0.286 nm and is consistent with the spacing distance between the (220) planes. The (001) plane is perpendicular to (220), as illustrated in Fig. 2c, so the surface exposed on the cube-shaped Co_3O_4 particles is the (001) plane. For comparison, the TEM micrograph of the commercial Co_3O_4 is shown in Fig. 2d, indicating the particle size of the commercial Co_3O_4 is around 100 nm.

Figure 3a shows the SEM images of the fuel cell fabricated using LSM–SDC– Co_3O_4 (cubes) as the cathode. The micrographs clearly show that the complete cell is composed of a three-layer structure, where the anode substrate supports the electrolyte layer. The electrolyte layer, which is approximately 30 μm in thickness, makes contact well with both the anode and cathode. Figure 3b shows the cathode layer of the cell. The Co_3O_4 nanocubes are dispersed on the

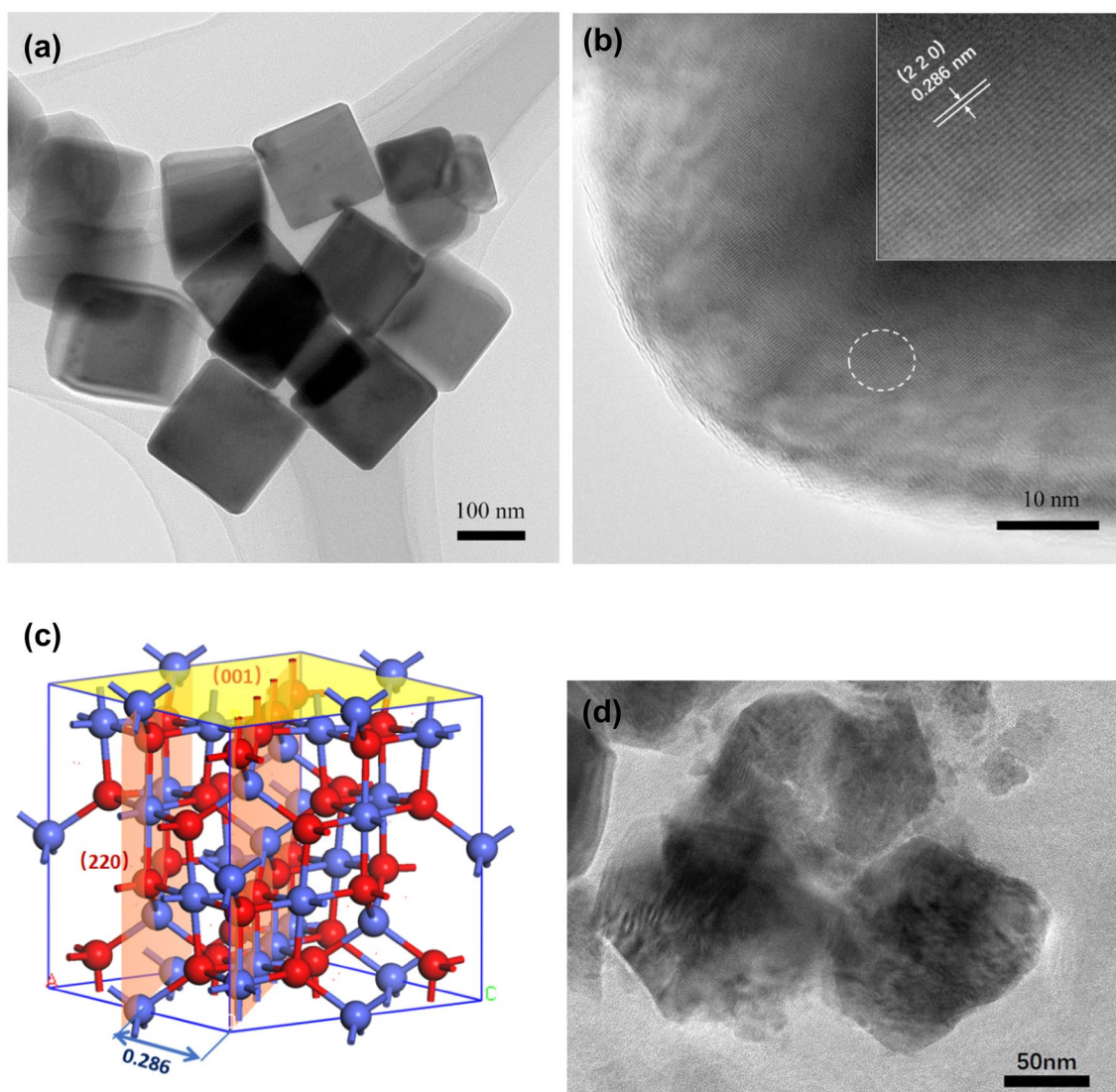


Fig. 2 **a** TEM images of Co_3O_4 nanocubes. **b** HRTEM of a Co_3O_4 nanocube. **c** Schematic of a (001) surface of Co_3O_4 nanocubes. **d** TEM images of commercial Co_3O_4 nanoparticles

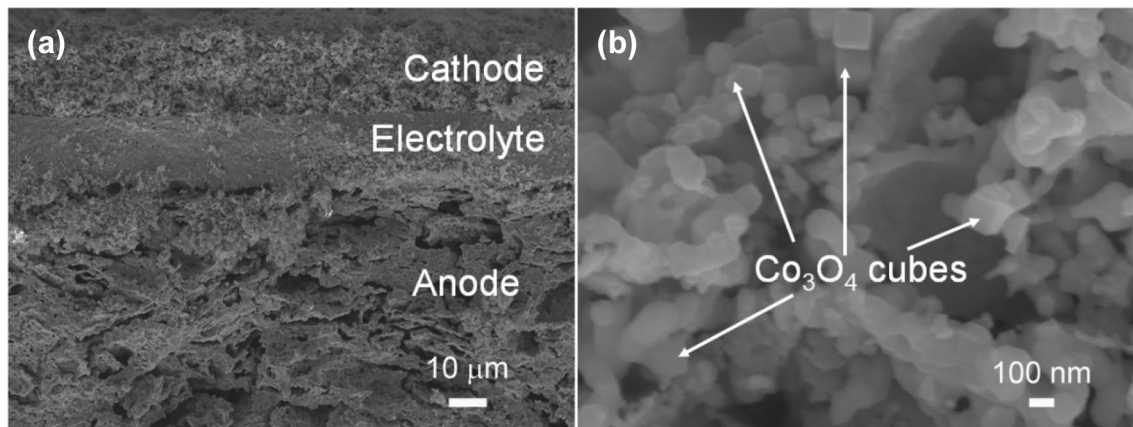


Fig. 3 SEM images of **a** the complete fuel cell and **b** an enlargement of the cathode

LSM20–SDC cathode, forming the LSM20–SDC– Co_3O_4 composite. Note that the particle size of the Co_3O_4 nanocubes in the cathode is still approximately 100–150 nm, and the Co_3O_4 particles maintain a cube shape, suggesting that the post thermal treatment at 800 °C in the fuel cell fabrication procedure does not obviously change the morphology or the size of the Co_3O_4 nanocubes.

Figure 4a shows the I–V and power density curves for the LSM20–SDC-based cell using Co_3O_4 nanocubes. The cell made using the Co_3O_4 nanocubes generated peak power densities of 152, 248, 500, 863 and 1126 mW cm^{-2} at 500, 550, 600, 650 and 700 °C, respectively. The power output of the cell made with Co_3O_4 nanocubes is significantly larger than that of the cell made with commercial Co_3O_4 nanoparticles, only reaching 179 mW cm^{-2} at 600 °C, as shown in Fig. 3b. Figure 3c shows the comparison of EIS plots for the cells made using the Co_3O_4 (001) plane nanocubes and commercial Co_3O_4 nanoparticles tested at 600 °C. The ohmic resistance (R_{ohmic}) and the polarization resistance (R_p) for the cell made with Co_3O_4 nanocubes are 0.11 and 0.27 $\Omega \text{ cm}^2$, respectively. In contrast, R_{ohmic} and R_p for the cell made with commercial Co_3O_4 nanoparticles are 0.18 and 0.8 $\Omega \text{ cm}^2$, respectively. These two cells have similar R_{ohmic} values, but the R_p values differ greatly. Although R_p is the sum of the anode polarization resistance and the cathode polarization resistance, these two cells were prepared in the same way, and the same anode composition was used for both of these cells, suggesting that the anode does not contribute significantly to R_p . In addition, it is generally recognized that the cathode is the major contributor to R_p [28], so the only difference between these two cells (either the use of Co_3O_4 (001) nanocubes or commercial Co_3O_4 nanoparticles) is the cause of the differing R_p values. The size of commercial Co_3O_4 particles (around 100 nm) is even smaller than that of the Co_3O_4 nanocubes (around 150 nm), suggesting the improvement in fuel cell performance is not due to the effect of the Co_3O_4 particles. Therefore, the

apparent differences in the cell performance and also the R_p values between the fuel cells made using Co_3O_4 (001) nanocubes and those made using commercial Co_3O_4 nanocubes mainly come from the utilization of the Co_3O_4 (001) surfaces, which is beneficial for the adsorption and dissociation of oxygen and thus favours the cathode reactions that are demonstrated in our theoretical simulations. Figure 4d shows the schemes of using Co_3O_4 nanocubes for LSM–SDC composite cathode. Due to the good ability of oxygen adsorption and dissociation at Co_3O_4 (001) surface, Co_3O_4 nanocubes allow a fast ORR to happen at the cathode, leading to a decreased R_p and then an improved fuel cell performance. Even compared to a similar LSM–SDC cathode composed of Co_3O_4 nanoarrays reported in a previous study [12], the Co_3O_4 (001) surface-based cathode fabricated in this study has a polarization resistance that is almost one order of magnitude lower, suggesting that the use of Co_3O_4 nanocubes would be a rational strategy for engineering Co_3O_4 nanostructures to boost the fuel cell performance. Although the LSM-based cells fabricated using the Co_3O_4 (001) surface-based cathode, as presented in this study, have improved performances compared to conventional LSM-based cells, decreased polarization resistances and increased performances compared to many LSM-based cells described in the literature [7, 29–31], the performance is still lower than that of cells made using highly active perovskite cathodes [32, 33]. Considering the pure electron-conducting nature of LSM compounds, further improvement in the fuel cell performance is reasonably expected by tailoring the cathode particle size or the size of the Co_3O_4 nanocubes to increase the number of active reaction sites [34–36], or by using an oxygen–electron mixed cathode instead of an LSM cathode [37–39]. It should be noted that although the mixed oxygen–electron conductors show better performance than LSM that makes them less influenced by the Co_3O_4 particles, the Co_3O_4 (001) surface has been demonstrated to promote the oxygen adsorption and dissociation that are critical steps for

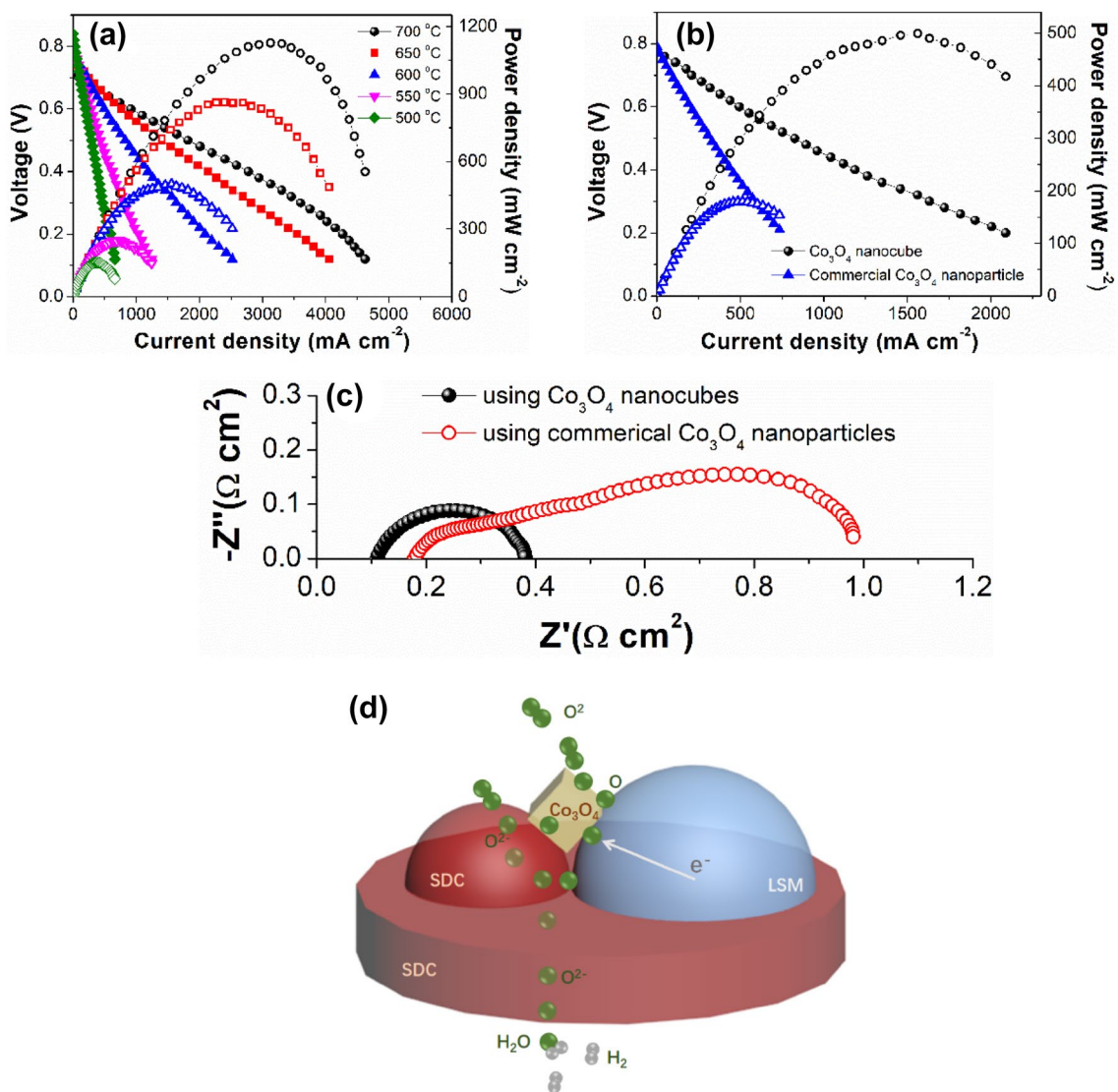


Fig. 4 **a** I–V and powder density curves for cells made using Co₃O₄ nanocubes. **b** Comparison of fuel cell performance with cathodes using Co₃O₄ nanocubes and commercial Co₃O₄ nanoparticles tested

at 600 °C. **c** Comparison of the EIS plots of the two cells tested at 600 °C. **d** Scheme of the use of Co₃O₄ nanocubes for the accelerated cathode reactions for SOFCs

cathode reactions. In addition, Co₃O₄ was found to promote the performance of the SOFC using Sm_{0.5}Sr_{0.5}CoO_{3-δ} cathode greatly [10], suggesting that the use of Co₃O₄ is still of great interest for mixed oxygen–electron conducting cathodes. Anyway, this study presents a new concept for using crystal planes to improve the oxide catalytic activity of SOFC cathode reactions, which provides a new way to design SOFC cathodes.

Conclusions

In this study, a new concept for using metal oxide nanocubes with specific exposed crystal planes in SOFC cathodes was provided. The theoretical simulations showed that the

Co₃O₄ (001) plane had better oxygen adsorption and oxygen dissociation, which improved the cathode reactions in the SOFCs. To validate the simulations, Co₃O₄ nanocubes with (001) planes exposed at the surface were synthesized and then used in the cathode of SOFCs. The cell performance was much improved with the use of the Co₃O₄ nanocubes with (001) surfaces compared with that of the cell using conventional Co₃O₄ nanoparticles. The EIS studies indicated that the utilization of Co₃O₄ nanocubes with exposed (001) surfaces accelerated the cathode reactions. This led to a smaller polarization resistance and thus a higher fuel cell performance, although the structure and compositions of the cells were similar. This study demonstrated the feasibility of tailoring and utilizing the exposed crystal planes of metal

oxides to enhance the performance of SOFC cathodes and may open new doors for the design of cathodes, which has not yet been revealed in the scientific community.

Acknowledgements This work was supported by the National Natural Science Foundation of China (Grant no. 51602238), the Natural Science Foundation of Shandong Province (Grant no. ZR2018JL017), the Startup Funding for Talents at Qingdao University (Grant no. 41117010097), the Thousand Talents Plan, the World-Class Discipline Program of Shandong Province and the Taishan Scholar's Advantageous and the Distinctive Discipline Program of Shandong Province, the China Postdoctoral Science Foundation (2017M622139) and the Qingdao Postdoctoral Application Research. The Australian Research Council (ARC) is also acknowledged for partially supporting this study under the ARC Laureate Fellowship Program (Project FL170100101).

Open Access This article is distributed under the terms of the Creative Commons Attribution 4.0 International License (<http://creativecommons.org/licenses/by/4.0/>), which permits unrestricted use, distribution, and reproduction in any medium, provided you give appropriate credit to the original author(s) and the source, provide a link to the Creative Commons license, and indicate if changes were made.

References

- Fan, L.D., Zhu, B., Su, P.C., He, C.X.: Nanomaterials and technologies for low temperature solid oxide fuel cells: recent advances, challenges and opportunities. *Nano. Energy*. **45**, 148–176 (2018)
- Xia, Y.P., Jin, Z.Z., Wang, H.Q., Gong, Z., Lv, H.L., Peng, R.R., Liu, W., Bi, L.: A novel cobalt-free cathode with triple-conduction for proton-conducting solid oxide fuel cells with unprecedented performance. *J. Mater. Chem. A*. **7**, 16136–16148 (2019)
- Chen, Y., Chen, Y., Ding, D., Ding, Y., Choi, Y., Zhang, L., Yoo, S., Chen, D.C., Deglee, B., Xu, H., Lu, Q.Y., Zhao, B.T., Vardar, G., Wang, J.Y., Bluhm, H., Crumlin, E.J., Yang, C.H., Liu, J., Yildiz, B., Liu, M.L.: A robust and active hybrid catalyst for facile oxygen reduction in solid oxide fuel cells. *Energ. Environ. Sci.* **10**(4), 964–971 (2017)
- Li, M., Chen, K.F., Hua, B., Luo, J.L., Rickard, W.D.A., Li, J., Irvine, J.T.S., Jiang, S.P.: Smart utilization of cobaltite-based double perovskite cathodes on barrier-layer-free zirconia electrolyte of solid oxide fuel cells. *J. Mater. Chem. A*. **4**(48), 19019–19025 (2016)
- Kilner, J.A., Burriel, M.: Materials for intermediate-temperature solid-oxide fuel cells. *Annu. Rev. Mater. Res.* **44**, 365–393 (2014)
- Saranya, A.M., Pla, D., Morata, A., Cavallaro, A., Canales-Vazquez, J., Kilner, J.A., Burriel, M., Tarancon, A.: Engineering mixed ionic electronic conduction in $\text{La}_{0.8}\text{Sr}_{0.2}\text{MnO}_3$ nanostructures through fast grain boundary oxygen diffusivity. *Adv. Energy Mater.* **5**(11), 1500377 (2015)
- Da'as, E.H., Bi, L., Boulfrad, S., Traversa, E.: Nanostructuring the electronic conducting $\text{La}_{0.8}\text{Sr}_{0.2}\text{MnO}_3$ cathode for high-performance in proton-conducting solid oxide fuel cells below 600 °C. *Sci. China Mater.* **61**(1), 57–64 (2018)
- Zhu, L., Wei, B., Wang, Z.H., Chen, K.F., Zhang, H.W., Zhang, Y.H., Huang, X.Q., Lue, Z.: Electrochemically driven deactivation and recovery in $\text{PrBaCo}_2\text{O}_5$ oxygen electrodes for reversible solid oxide fuel cells. *Chemosuschem.* **9**(17), 2443–2450 (2016)
- Chen, K.F., Li, N., Ai, N., Li, M., Cheng, Y., Rickard, W.D.A., Li, J., Jiang, S.P.: Direct application of cobaltite-based perovskite cathodes on the yttria-stabilized zirconia electrolyte for intermediate temperature solid oxide fuel cells. *J. Mater. Chem. A*. **4**(45), 17678–17685 (2016)
- Zhang, H.Z., Liu, H.Y., Cong, Y., Yang, W.S.: Investigation of $\text{Sm}_{0.5}\text{Sr}_{0.5}\text{CoO}_3/\text{Co}_3\text{O}_4$ composite cathode for intermediate-temperature solid oxide fuel cells. *J. Power. Sources*. **185**(1), 129–135 (2008)
- Zhang, C.J., Du, Z.H., Zhao, H.L., Zhang, X.X.: Modification of electrocatalytic activity of $\text{BaCe}_{0.4}\text{Sm}_{0.2}\text{Fe}_{0.4}\text{O}_3$ with Co_3O_4 as cathode for proton-conducting solid oxide fuel cell. *Electrochim. Acta*. **108**, 369–375 (2013)
- Li, M.M., Cheng, J.G., Gan, Y., Xu, C.X.: In situ construction of Co_3O_4 nanoarray catalysts on $(\text{La}_{0.8}\text{Sr}_{0.2})_{0.95}\text{MnO}_3$ cathode for high-efficiency intermediate-temperature solid oxide fuel cells. *Ceram. Int.* **44**(3), 3472–3479 (2018)
- Hu, L.H., Peng, Q., Li, Y.D.: Selective synthesis of Co_3O_4 nanocrystal with different shape and crystal plane effect on catalytic property for methane combustion. *J. Am. Chem. Soc.* **130**(48), 16136 (2008)
- Xiao, X.L., Liu, X.F., Zhao, H., Chen, D.F., Liu, F.Z., Xiang, J.H., Hu, Z.B., Li, Y.D.: Facile shape control of Co_3O_4 and the effect of the crystal plane on electrochemical performance. *Adv. Mater.* **24**(42), 5762–5766 (2012)
- Xie, X.W., Li, Y., Liu, Z.Q., Haruta, M., Shen, W.J.: Low-temperature oxidation of CO catalysed by Co_3O_4 nanorods. *Nature*. **458**(7239), 746–749 (2009)
- Hohenberg, P., Kohn, W.: Inhomogeneous electron gas. *Phys. Rev.* **136**(3B), B864 (1964)
- Blöchl, P.E., Jepsen, O., Andersen, O.K.: Improved tetrahedron method for Brillouin-zone integrations. *Phys. Rev. B*. **49**(23), 16223 (1994)
- Kresse, G., Furthmüller, J.: Efficient iterative schemes for ab initio total-energy calculations using a plane-wave basis set. *Phys. Rev. B*. **54**(16), 11169–11186 (1996)
- Payne, M.C., Teter, M.P., Allan, D.C., Arias, T., Joannopoulos, A.J.: Iterative minimization techniques for ab initio total-energy calculations: molecular dynamics and conjugate gradients. *Rev. Mod. Phys.* **64**(4), 1045 (1992)
- Anisimov, V.I., Zaanen, J., Andersen, O.K.: Band theory and Mott insulators: Hubbard U instead of stoner I. *Phys. Rev. B*. **44**(3), 943 (1991)
- Anisimov, V.I., Aryasetiawan, F., Lichtenstein, A.: First-principles calculations of the electronic structure and spectra of strongly correlated systems: the LDA+U method. *J. Phys.* **9**(4), 767 (1997)
- Materials project. <http://www.materialsproject.org>
- Henkelman, G., Uberuaga, B.P., Jónsson, H.: A climbing image nudged elastic band method for finding saddle points and minimum energy paths. *J. Chem. Phys.* **113**(22), 9901–9904 (2000)
- Zhang, Y.X., Ding, F., Deng, C., Zhen, S.Y., Li, X.Y., Xue, Y.F., Yan, Y.M., Sun, K.N.: Crystal plane-dependent electrocatalytic activity of Co_3O_4 toward oxygen evolution reaction. *Catal. Commun.* **67**, 78–82 (2015)
- Wang, B., Liu, X.H., Bi, L., Zhao, X.S.: Fabrication of high-performance proton-conducting electrolytes from microwave prepared ultrafine powders for solid oxide fuel cells. *J. Power. Sources*. **412**, 664–669 (2019)
- Ding, X.F., Gao, Z.P., Ding, D., Zhao, X.Y., Hou, H.Y., Zhang, S.H., Yuan, G.L.: Cation deficiency enabled fast oxygen reduction reaction for a novel SOFC cathode with promoted CO_2 tolerance. *Appl. Catal. B-Environ.* **243**, 546–555 (2019)
- Liu, M., Liu, J.J., Li, Z.L., Wang, F.: Atomic-level Co_3O_4 layer stabilized by metallic cobalt nanoparticles: a highly active and stable electrocatalyst for oxygen reduction. *ACS. Appl. Mater. Inter.* **10**(8), 7052–7060 (2018)
- Peng, R.R., Wu, T.Z., Liu, W., Liu, X.Q., Meng, G.Y.: Cathode processes and materials for solid oxide fuel cells with proton conductors as electrolytes. *J. Mater. Chem.* **20**(30), 6218–6225 (2010)

29. Sadykov, V., Alikina, G., Lukashevich, A., Muzykantov, V., Usoltsev, V., Boronin, A., Koscheev, S., Krieger, T., Ishchenko, A., Smirnova, A., Bobrenok, O., Uvarov, N.: Design and characterization of LSM/ScCeSZ nanocomposite as mixed ionic-electronic conducting material for functionally graded cathodes of solid oxide fuel cells. *Solid. State. Ion.* **192**(1), 540–546 (2011)
30. Zhang, L., Zhao, F., Peng, R.R., Xia, C.R.: Effect of firing temperature on the performance of LSM–SDC cathodes prepared with an ion-impregnation method. *Solid. State. Ion.* **179**(27–32), 1553–1556 (2008)
31. Choi, J.J., Oh, S.H., Noh, H.S., Kim, H.R., Son, J.W., Park, D.S., Choi, J.H., Ryu, J., Hahn, B.D., Yoon, W.H., Lee, H.W.: Low temperature fabrication of nano-structured porous LSM-YSZ composite cathode film by aerosol deposition. *J. Alloy. Compd.* **509**(5), 2627–2630 (2011)
32. Sumi, H., Yamaguchi, T., Hamamoto, K., Suzuki, T., Fujishiro, Y.: High performance of $\text{La}_{0.6}\text{Sr}_{0.4}\text{Co}_{0.2}\text{Fe}_{0.8}\text{O}_3\text{-Ce}_{0.9}\text{Gd}_{0.1}\text{O}_{1.95}$ nanoparticulate cathode for intermediate temperature microtubular solid oxide fuel cells. *J. Power. Sources.* **226**, 354–358 (2013)
33. Wachsman, E., Ishihara, T., Kilner, J.: Low-temperature solid-oxide fuel cells. *MRS. Bull.* **39**(9), 773–782 (2014)
34. Zhang, X.M., Liu, L., Zhao, Z., Tu, B.F., Ou, D.R., Cui, D.A., Wei, X.M., Chen, X.B., Cheng, M.J.: Enhanced oxygen reduction activity and solid oxide fuel cell performance with a nanoparticles-loaded cathode. *Nano. Lett.* **15**(3), 1703–1709 (2015)
35. Xu, X., Bi, L., Zhao, X.S.: Highly-conductive proton-conducting electrolyte membranes with a low sintering temperature for solid oxide fuel cells. *J. Membr. Sci.* **558**, 17–25 (2018)
36. Sun, Z.Q., Liao, T., Kou, L.Z.: Strategies for designing metal oxide nanostructures. *Sci. China. Mater.* **60**(1), 1–24 (2017)
37. Bi, L., Shafi, S.P., Da'as, E.H., Traversa, E.: Tailoring the cathode-electrolyte interface with nanoparticles for boosting the solid oxide fuel cell performance of chemically stable proton-conducting electrolytes. *Small* **14**(32), 1801231 (2018)
38. Xu, X., Wang, H.Q., Ma, J.M., Liu, W.Y., Wang, X.F., Fronzi, M., Bi, L.: Impressive performance of proton-conducting solid oxide fuel cells using a first-generation cathode with tailored cations. *J. Mater. Chem. A.* **7**, 18792–18798 (2019)
39. Dong, F.F., Chen, Y.B., Ran, R., Chen, D.J., Tade, M.O., Liu, S.M., Shao, Z.P.: $\text{BaNb}_{0.05}\text{Fe}_{0.95}\text{O}_3$ as a new oxygen reduction electrocatalyst for intermediate temperature solid oxide fuel cells. *J. Mater. Chem. A.* **1**(34), 9781–9791 (2013)

Publisher's Note Springer Nature remains neutral with regard to jurisdictional claims in published maps and institutional affiliations.